Journal of the Ceramic Society of Japan 116 [7] 803-806 2008 **Paper**

Ionic conductivity of $Li_xLa_{10-x}(SiO_4)_6O_{3-x}$ sinters

Naoki TAKEDA, Yoshiteru ITAGAKI and Yoshihiko SADAOKA

Department of Materials Science and Biotechnology, Graduate School of Science and Engineering, Ehime University, 3, Bunkyo-cho, Matsuyama 790−8577

A series of Li_2O–La_2O_3–SiO_2 sinters were prepared with the various ratios of the associated elements, Li: La: Si = x: (10–x): 6, and their ionic conductivities were examined. All the sinters were mainly composed of the apatite-type $Li_xLa_{10-x}(SiO_4)_6O_{3-x}$ crystalline phases but sub-phases were produced in some cases. The lattice parameters of the main phase decreased with an increase in the Li-content, x, up to x = 2.0 and became constant above x = 2.0, indicating that La 4f-site was partially replaced by Li up to the maximum of x = 2.0. The conductivity of the sinters gradually increased with an increase in x to 1.5, but it suddenly dropped down at x = 2.0 and increased again by a further increase in x. The XRD and ^{29}Si-NMR results suggested that the first conductivity increase was due to the decrease in the content of the La_2SiO_5 sub-phase with the Li replacement. Furthermore, the ^{7}Li-NMR measurements gave evidence that lithium silicate sub-phase was formed at above x = 2 in the grain-boundary of the crystalline phase as a high Li-ionic conducting phase. The Nernst's EMF response of the O_2 and CO_2 concentration cells suggested that the main ionic carriers were oxide ion at x < 2.0 and lithium ion at $x \geq 2$.

Key-words : Lithium lanthanum silicate, Apatite-type crystal, Iionic conductor, ^{7}Li-NMR, ^{29}Si-NMR, XRD

[Received January 10, 2008; Accepted May 15, 2008]

1. Introduction

Lanthanoid silicates with an apatite structure, $La_{9.33+x}(SiO_4)_6O_{2+3x/2}$, are known as good oxide ion conductors.[1),2)] Some of those exhibit even higher conductivity than that of yittria stabilized zirconia (YSZ) which is the commodity type of oxide ion conductor. Therefore the lanthanoid silicates are expected as a new solid electrolyte material for SOFC and sensor devices, etc.

Meanwhile, new classes of lithium ionic conductors formulated by $LiLnSiO_4$ (Ln = lanthanoids) and related materials were also reported.[3)–5)] The product from the mixture with an elemental ratio of Li: Ln: Si = 1: 1: 1 was mainly composed of an apatite phase, $Li_xLa_{10-x}(SiO_4)_6O_{3-x}$, analogous to the $La_{9.33+x}(SiO_4)_6O_{2+3x/2}$. In 1993, as the part of a screening program for dense and ionic conductive solid-state electrolytes, the electrical properties of a series of rare earth silicates, M_2O–Ln_2O_3–$2SiO_2$ (M = alkali metals) had been studied.[3)] The observed XRD patterns for Ln = La, Nd, Sm, Gd and Dy, were very similar to that of $LiLaSiO_4$ or $LiLa_9(SiO_4)_6O_2$ with an apatite structure (hexagonal, $P6_3/m$). Structure types of lithium lanthanoid silicates were reported by Blasse et al.[6)] According to their report, the compounds with large lanthanoid ions from La to Dy belong to hexagonal, and those with the small lanthanoid ions belong to orthorhombic. Sato et al.[7)] proposed that the lithium ion conductivities of the sinters were found to consist of two contributions: one was the grain boundary composed of lithium silicate amorphous phase and the other was the bulk phase with an apatite structure. For Ln = La system, the conductivity of phase boundary was higher and the activation energy was lower than those of the bulk phase.[7)] It is thus evident that the sub-phases comprised in the sinters significantly contribute to the conduction behaviors. Therefore such the sub-phases should be directly detected with some suitable approaches. In this work, a series of lithium lanthanum silicates with different lithium contents were prepared and their conduction change with the lithium content were investigated based on the phase compositions by means of XRD, ac-impedance analysis and solid-state ^{7}Li- and ^{29}Si-NMR techniques.

2. Experimental

$Li_xLa_{10-x}(SiO_4)_6O_{3-x}$ was prepared from the solid-state mixture of Li_2CO_3, La_2O_3 and SiO_2 in the prescribed ratios by heating at 1000°C in an ambient atmosphere with a box furnace. The cooled samples were ball-milled, compacted into disks and then heated again at several temperatures in the ambient atmosphere. The ac conductivities of the sinters in disks were determined in ambient air by using impedance/gain-phase analyzer (Hewlett-Packard, 4194A) in a frequency region between 100 Hz and 15 MHz. The sinters in powders were examined with XRD (Kα-Cu, Rigaku RINT2200V), solid-state ^{29}Si-NMR (JEOL JNM-CMX300) at 59.74 MHz (rotation: 4 kHz) and ^{7}Li-NMR at 116.86 MHz. Chemical shifts are quoted relative to polydimethylsilane and lithium chloride, respectively.

3. Results and discussion

The lithium lanthanum silicates were prepared with the various feed ratios of the associated elements, Li: La: Si = x: (10–x): 6, and sintered at different temperatures between 1100–1600°C. **Figure 1** shows the XRD powder patterns of the sinters with the Li contents of x = 0–4 measured at RT. Since the addition of Li-element tends to decrease the melting points of the silicates, the sintering temperature could be concomitantly lowered for those with higher Li-contents. The XRD of x = 0 suggested the formations of $La_{9.33}(SiO_4)_6O_2$ main phase and La_2SiO_5 sub-phase. The main phase of $La_{9.33}(SiO_4)_6O_2$ deviates in its composition from the feed ratio, having 6.7% vacancy at the La site. It is possible that redundant La ions form the sub-product. However, with an increase in Li-content, x, signal intensity of the La_2SiO_5 sub-phase decreased and the signals of the main product shifted to a higher value of 2θ. Such the peak position shift was not observed for the samples of $x \geq 2$. The lattice parameters of

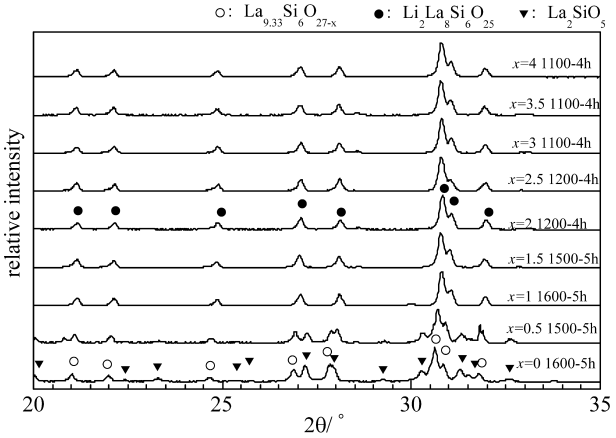

Fig. 1. XRD patterns of a series of the Li_2O–La_2O_3–SiO_2 sinters with the various feed ratios of the associated elements, Li: La: Si = x: (10–x): 6 ($0 \le x \le 4$). The sintering temperatures are denoted in the Fig.

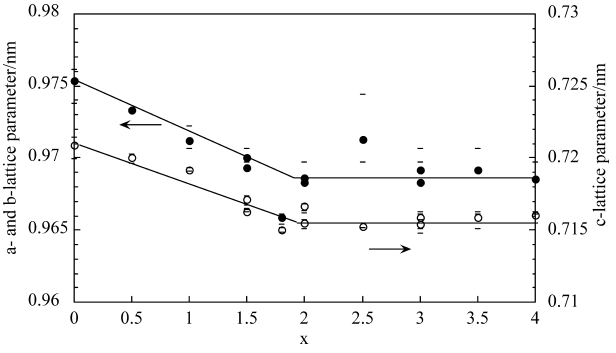

Fig. 2. Lattice parameter change of the $Li_xLa_{10-x}(SiO_4)_6O_{3-x}$ phases (assuming an apatite structures with hexagonal P–3) with the change in the lithium contents, x.

the main products were determined based on an apatite structures with hexagonal P–3 (ICSD: 94315) for $La_{9.33}(SiO_4)_6O_2$, $La_{4.67}(SiO_4)_3O$ and $P6_3/m$ (ICSD: 30585 and 83279) for $Li_2La_8(SiO_4)_6O$. The evaluated lattice parameters for the different x-values are shown in **Fig. 2**. The lattice parameters decreased with an increase in the Li-content, x, and became constant from $x = 2.0$ to 4.0. The decrease in the parameters suggests the partial replacement of La ions at 4f-sites with smaller Li ions.

Some workers[8),9)] studied on the ^{29}Si-NMR isotropic chemical shifts of the series of the solid silicates. The ^{29}Si-NMR chemical shifts of the silicates are observable in the range between –60 and –120 ppm with well-separated ranges for monosilicates (Q_0), disilicates and chain end groups (Q_1), middle groups in chains (Q_2), chain branching sites (Q_3), and the three-dimensional cross-linked framework (Q_4). Therefore, ^{29}Si-NMR can be a good approach to evaluate phase homogeneity of the sinters. The ^{29}Si-NMR data for the series of lithium lanthanum silicates are summarized in **Table 1**. Only singlet ^{29}Si-peaks were observed for all the lanthanum silicates at around –77.4 ppm even when Si is partially replaced by Al,[10)] indicating that the $[SiO_4]^{4-}$ units are chemically equivalent. The values of chemical shifts seem to belong to the Q_0 or Q_1 sub-divisions where the $[SiO_4]^{4-}$ is almost isolated. The ^{29}Si chemical shifts of the main phases were nearly the same for the series of the silicates, suggesting that the Li-substitution did not affect the structure of the $[SiO_4]^{4-}$ tetrahedra. In the case of $La_{10}(SiO_4)_6O_3$ and $La_{9.33}(SiO_4)_6O_2$, two kinds of chemical shifts for the La_2SiO_5 sub-phase were observed in the region > –80 ppm. This deviation of the chemical shift is probably due to the distortions and/or displacements in some of the $[SiO_4]^{4-}$ units arising from cation vacancies. Although the La_2SiO_5 phase is hardly detected at $x > 0.5$ by XRD, the NMR result unambiguously suggests that the sub-phase exists at $x \le 1.5$.

The ^{7}Li isotropic chemical shifts in the series of sinters were

Table 1. Solid-state ^{29}Si- and ^{7}Li-NMR Data of Lanthanum Silicates and Lithium Lanthanum Silicates

Samples	^{29}Si-NMR		^{7}Li-NMR		Products
	Chemical shift (ppm)	Relative intensities (%)	Chemical shift (ppm)	Relative intensities (%)	
$La_{10}(SiO_4)_6O_3$	–77.8, –82.4, –85.4	43.6, 49.0, 7.4	–	–	–
$La_{9.33}(SiO_4)_6O_2$	–77.1, –82.2, –85.8	68.7, 26.4, 4.9	–	–	–
$Li_xLa_{10-x}(SiO_4)_6O_{3-x}$					
$x = 0.5$	–77.6, –81.5	78.2, 21.8	0.019, 3.5	75.2, 24.8	$Li_{0.5}La_{9.5}(SiO_4)_6O_{2.5}$, La_2SiO_5, Li_2O
$x = 1.0$	–77.4, –80.5	86.4, 13.6	–0.086, 3.6	63.5, 36.5	$LiLa_{9.0}(SiO_4)_6O_{2.0}$, La_2SiO_5, Li_2O
$x = 1.5$	–77.7, –81.3	83.5, 16.5	0.025, 3.7	91.9, 8.1	$Li_{1.5}La_{8.5}(SiO_4)_6O_{1.5}$, La_2SiO_5, Li_2O
$x = 2.0$	–77.3	100	–0.220, 1.7	88.5, 11.5	$Li_{2.0}La_{8.0}(SiO_4)_6O$, Lithium silicates
$x = 2.5$	–77.5	100	–0.230, 1.7	90.8, 9.2	$Li_{2.0}La_{8.0}(SiO_4)_6O$, Lithium silicates
$x = 3.0$	–77.1	100	–0.130, 1.8	76.7, 23.3	$Li_{2.0}La_{8.0}(SiO_4)_6O$, Lithium silicates
$x = 3.5$	–77.2	100	–0.150, 1.8	76.1, 23.9	$Li_{2.0}La_{8.0}(SiO_4)_6O$, Lithium silicates
$x = 4.0$	–77.3	100	–0.150, 1.7	76.5, 23.5	$Li_{2.0}La_{8.0}(SiO_4)_6O$, Lithium silicates
$La_{9.83}Si_{4.5}Al_{1.5}O_{26}$	–77.6	100	–	–	Ref. 10
La_2SiO_5	–83.3	100	–	–	–
Li_2SiO_3	–64.5	100	1.14	100	–
Li_4SiO_4	–62.9	100	2.33	100	–
Li_2O	–	–	2.7	100	Ref. 11

also examined. Two kinds of ^{7}Li-signals appeared at around 0 ppm and at a higher chemical shift, and the intensity of the former peaks was much higher than that of the latter peaks. The intense former signals are attributable to the ^{7}Li nucleus of the apatite phases and their chemical shift does not depend on the x-values. The weaker signals appeared at around 3.6 ppm up to $x \leq 1.5$, but intensities of those signals decreased with an increase in x. This chemical shift might be assigned to Li_2O (2.7 ppm)[11] or other related compounds, which can be produced by the recombination between Li^+ and O^{2-} ions. At $x \geq 2.0$ the signals were detected in the range of 1.7–1.8 ppm. These chemical shifts are close to the lithium metasilicate, Li_2SiO_3 (1.14 ppm) and/or lithium orthosilicate, Li_4SiO_4 (2.33 ppm). By increasing x from 2.0, the relative intensity of the signal observed at higher chemical shift was increased to 23.3–23.9%. The ^{29}Si-NMR signal of a pure Li_2SiO_3 was weakly detected at 64.5 ppm, but the signal was too weak to detect for the samples of $x \geq 2$. Since Li ion can occupy the La 4f-site up to the maximum of $x = 2$, the excess amount of Li produces the sub-phase of Li_2SiO_3. The observed solid NMR spectra of ^{29}Si and ^{7}Li nuclei suggested that the sinters are composed of La_2SiO_5 and apatite-phase $Li_xLa_{10-x}(SiO_4)_6O_{3-x}$ for $x < 2$ and Li_2SiO_3 and apatite-phases for $x \geq 2$.

The expected crystal structures with an hexagonal of $La_{9.33}(SiO_4)_6O_2$ (P–3) and $Li_2La_8(SiO_4)_6O$ ($P6_3/m$) are shown in **Fig. 3**. The observed XRD pattern of the sinters with $La_{9.33}(SiO_4)_6O_2$ and $Li_2La_8(SiO_4)_6O$ compositions agreed well with the ICSD files for $La_{4.67}(SiO_4)_3O$ and $Li_2La_8(SiO_4)_6O$, respectively. The decrease in the lattice parameters from $x = 0$ to 2 is due to the partial replacement of La at the 4f-sites with Li ion. According to the published results, which appeared in the ICSD files, the structure of $La_{4.67}(SiO_4)_3O$ consists of the isolated SiO_4 tetrahedra with the remaining oxygen being present as O^{2-} ions at 2a-sites in one-dimensional tunnels running parallel to the c-axis. There are two kinds of La sites, La (6h) and La (4f), and the former is fully occupied and the latter is partially occupied. The structure of $Li_2La_8(SiO_4)_6O$ is very similar to that of $La_{4.67}(SiO_4)_3O$. The occupancies of the 4f-site with Li and La are 20 and 80%, respectively. Meanwhile, the occupancy of the 2a-site with O^{2-} is *ca*, 92%. These structures suggest that in both crystals, oxide ions situated at 2a-sites are mobile along the c-axes.

The electrical conductivity of the sinters in ambient air was determined with ac-impedance analysis. In the complex impedance plots, arcs and spike were observed in a high and low frequency ranging from 10 MHz to 100 Hz. The total resistances were determined from the intercept of the spikes and/or the arcs in the lower frequency end on the Z axis. The relationships between logarithm of the conductivity (G) and the reciprocal absolute temperature ($1/T$) are shown in **Fig. 4**. In all the cases,

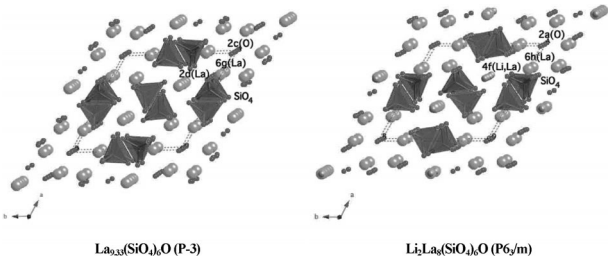

Fig. 3. Expected crystal structures of $La_{9.33}(SiO_4)_6O_2$ and $Li_2La_8(SiO_4)_6O$ with hexagonal P–3 and $P6_3/m$, respectively.

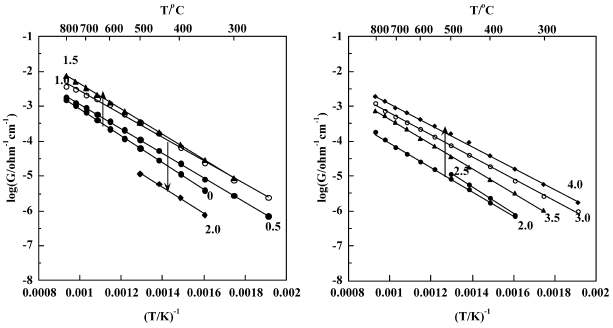

Fig. 4. Relationships between logarithm of the conductivity (G) and the reciprocal absolute temperature ($1/T$) for the Li_2O–La_2O_3–SiO_2 sinters with the lithium contents (a) $0 \leq x \leq 2$ and (b) $2.5 \leq x \leq 4$.

the relationship was well expressed by the Arrhenius Eq.:

$$G = G_0 \exp(-\Delta E/kT) \quad (1)$$

where G_0, ΔE and k are pre-exponential factor, activation energy and Boltzmann constant, respectively. **Figure 5** demonstrates the conductivity change at 500°C with the change in the Li-content. The conductivity change can be classified into two ranges of x; one is $0 \leq x \leq 1.5$ and the other is $2 \leq x \leq 4$. For each range of x, logarithm of the conductivities linearly increased with the increase in the Li-content. From the XRD and NMR results, the first increase in the conductivity is possibly due to the decrease in the lower conductive La_2SiO_5 phase which completely disappeared at $x = 1.5$. Since $x = 0$ is known as an oxide ion conductor, it is deduced that the occurring phenomenon is an increase in oxide ion conductivity. In spite of the absence of the La_2SiO_5 phase, the conductivity suddenly dropped at $x = 2$. The ^{7}Li-NMR data unambiguously indicated the formation of the new phase: that is Li_2SiO_3, at $x \geq 2$. It is possible that the recombination of

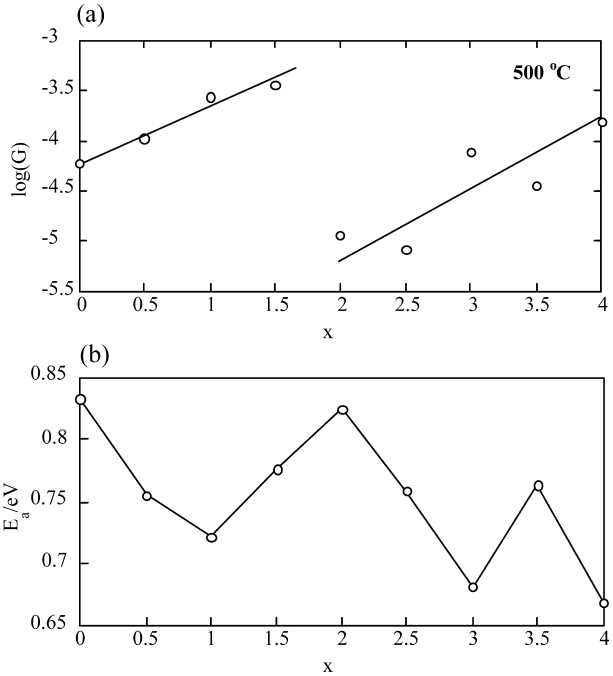

Fig. 5. Conductivity at 500°C (a) and activation energy (b) changes of the Li_2O–La_2O_3–SiO_2 sinters with different Li-contents.

mobile oxide and lithium ions originated from the lithium silicate reduces the whole conductivity to a minimum. At $x \geq 2$, the lithium silicate sub-phase increases with the increase in the Li-content and this causes the lithium ion conductivity. Pernice et al.[12] previously reported the high Li ion conductivity of Li_2SiO_3 glass, that was more than 10^{-2} Scm^{-1} at 500°C and the activation energy was 0.52 eV. They also reported that Li_4SiO_4 transformation in Li_2SiO_3 by heating reduced the conductivity and increased the activation energy to 0.97 eV. The activation energy change is shown in Fig. 5. The activation energy first increased and came to its maximum at $x = 2$ (0.83 eV). After that the activation energy decreased and finally reached to 0.67 eV. This decrease in the activation energy at $x \geq 2$ is probably due to the formation of the lithium silicate sub-phase having the low activation energy. Since the activation energy of Li_4SiO_4 is large, the sub-phase could be mainly composed of Li_2SiO_3. Because the lattice parameter change indicated that $x = 2$ was the maximal lithium composition in the apatite phase, $Li_xLa_{10-x}(SiO_4)_6O_{3-x}$, the separated Li_2SiO_3 phase may exist at the grain boundary of the $Li_2La_8(SiO_4)_6O$ crystalline phase.

The mobile ionic species was more directly confirmed by measuring the Nernstian electron motive force (EMF). For this purpose, some structures of a gas sensor were constructed. First, the sinters in disc are applied to a potentiometric O_2 sensor. The potentiometric O_2 sensor using an oxygen ionic electrolyte is expressed as (I)O_2, Pt/oxygen ionic electrolyte/Pt, ref. (II). The output signal (EMF) in volt is controlled by the difference of the oxygen concentration between the sensing and reference electrodes,

$$E_{obs} = E_o + (RT/nF)\ ln\ (P_{O2(I)}/P_{O2(II)}) \qquad (2)$$

and the electron number, n, is 4 for the transport number of oxygen is unity. The response behaviors at 550°C are shown in **Fig. 6**. In ca, 20 min intervals, the test gas was changed in a stepwise in the range of 21% and 0% (high purity nitrogen). It was confirmed that the response and recovery times were shortened with an increase in the operating temperature. The output EMF was proportional to the logarithm of the O_2 concentration and the estimated electron number, n, was approximately 4 for $x = 0$ and 1. This indicates that the transport numbers of these sinters is unity and they are pure oxide ion conductors. With an increase in x to 2 and 3, the estimated electron number decreased to around 3.3 and 2.5, respectively. This indicates the contribution of ionic species other than the oxide ion, possibly that is Li^+ ion acting as an ionic carrier for $x > 2.0$. The devices with Pt, Li_2CO_3/sinter/Pt structure were also constructed and the response to CO_2 gas was examined. In this case an electron number $n = 2$ means the transport number is unity. The device constructed with the sinter of $x = 2.0$ responded to CO_2 with 2 in the electron number, but didn't respond for $x = 0$ and 1.0. This result unambiguously indicates that Li ion conduction is dominant and sufficiently high for a good response to CO_2 at $x = 2$ and larger.

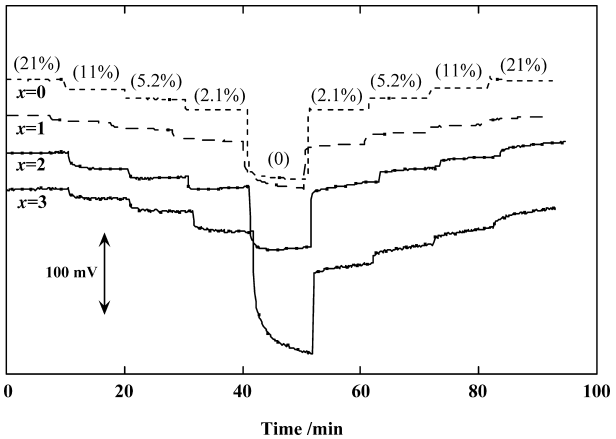

Fig. 6. Response to the change in O_2 concentration examined at 550°C for the elements with Pt/sinters/Pt structure, where the sinters are $x = 0$, 1, 2 and 3. The oxygen concentrations in % are indicated in parentheses.

4. Conclusion

The Li–La–Si–O sinters with various Li contents were prepared and their conductivities were investigated. For $x \leq 1.5$, the sinter was mainly composed of the apatite structures but the sub-product of La_2SiO_5 coexisted. By adding the Li-element, the $Li_xLa_{10-x}(SiO_4)_6O_{3-x}$ phase appeared with the partial replacement of La–4f site together with a decrease in the La_2SiO_5 sub-phase. With an increase in the Li-content, the lattice parameters decreased up to $x = 2$ and became constant at $x \geq 2$, suggesting that the replacement of the La sites with Li ions occurred up to $x = 2$. The ^{29}Si and ^{7}Li solid NMR spectra analyses suggested that the sinters were composed with some phases, such as La_2SiO_5, and apatite-type Li–La–Si–oxides for $x < 2$ and Li_2SiO_3 and apatite-type Li–La–Si–oxides for $x > 2$. It was concluded that the ionic conductivity was strongly influenced by the sub-products. The conduction behavior of the oxides can be classified into two groups. In the range $0 \leq x \leq 1.5$, oxide ion conductivity increased with an increase in the Li-contents due to the decrease in the La_2SiO_5. On the other hand, in the range $2.0 \leq x \leq 4.0$, lithium ion conductivity was induced with the existence of the Li_2SiO_3 phase. It was thus clarified that the ionic conductivity of the Li–La–Si–O sinters can be controlled with a change in the Li-content.

References

1) S. Nakayama and M. Sakamoto, *J. Eur. Ceram. Soc.*, **18**, 1413–1418 (1998).
2) P. R. Slater, J. E. H. Sansom and J. R. Tolchard, *Chem. Rec.*, **4**, 373–384 (2004).
3) S. Nakayama and Y. Sadaoka, *J. Mater. Chem.*, **3**, 1251–1257 (1993).
4) H. Matsumoto, K. Yonezawa and H. Iwahara, *Solid State Ionics*, **113–115**, 79–87 (1998).
5) Y. Sadaoka, S. Nakayama, Y. Sakai and M. Wake, *Sensors and Actuators B*, **24–25**, 282–286 (1995).
6) G. Blasse and J. de Vries, *J. Inorg. Nucl. Chem.*, **29**, 1541–1542 (1967).
7) M. Sato, Y. Kono, H. Ueda, K. Uematsu and K. Toda, *Solid State Ionics*, **83**, 249–256 (1996).
8) E. Lippmaa, M. Maegi, A. Samson, G. Engelhard and A.-R. Grimmer, *J. Am. Chem. Soc.*, **102**, 4889–4893 (1980).
9) J. E. H. Sansom, J. R. Tolchard, M. S. Islam, D. Apperley and P. R. Slater, *J. Mater. Chem.*, **16**, 1410–1413 (2006).
10) N. Takeda, Y. Itagaki and Y. Sadaoka, *J. Ceram. Soc. Japan*, **115**, 643–647 (2007).
11) T. R. Krawietz, D. K. Murray and J. F. Haw, *J. Phys. Chem.*, **102**, 8779–8785 (1998).
12) P. Pernice, A. Aronne and A. Marotta, *Solid State Ionics*, **37**, 79–81 (1989).